Chapter 7

In Vitro Evolution of RNA Binding Peptides for Increased Specificity

Abstract

The Hepatitis C Virus internal ribosme entry site (HCV IRES) is an attractive target for inhibition of HCV translation. Using peptides that we selected to bind P6.1, a domain of human telomerase RNA, we perform mutagenic PCR and additional cycles of selection to isolate sequences that bind to P6.1 and to domain IIId of the HCV IRES. The P6.1-binding sequences are highly specific for their target but the HCV IIId-binding sequences bind to both P6.1 and domain IIId. Our data show that although only a few positions are necessary for RNA binding specificity, these mutations are relatively rare.

Introduction

Hepatitis C Virus (HCV) infects nearly 170 million people worldwide, of which 75-85% are chronically infected (1). HCV can cause liver cirrhosis and hepatocellular carcinoma, however most individuals are asymptomatic. Pegylated interferon and ribavirin are currently used to treat HCV, but are only 40-80% effective in all patients (2). Like the human immunodeficiency virus (HIV), HCV mutates rapidly and becomes resistant to drugs targeting viral enzymes (2).

The 5' end of the HCV genome, however, is relatively well conserved among isolated strains of HCV (3). The 5' untranslated region (UTR) folds into an internal ribosome entry site (IRES) that allows cap-independent translation of the HCV genome. The HCV IRES binds to the 40S ribosomal subunit (K_d= 2 nM) as well as the initiation factor eIF3 (K_d= 35 nM) (4). The high conservation seen in the IRES region is most likely due to the fact that it needs to interact with these cellular components.

Because of its high conservation, the HCV IRES, represents a good target for inhibition of HCV. The secondary structure of HCV has been determined (Figure 7.1) and contains four conserved domains. Domains II, IIIc-f, and IV interact with the 40S subunit (5-7) while domains IIIa and IIIb interact with eIF3 (8, 9). These domains have been targeted using ribozymes, RNA aptamers, and antisense oligos (10) and most inhibit IRES-mediated translation *in vitro*, validating the HCV IRES as a potential drug target.

Using mRNA display, we have previously selected RNA binding peptides that bind with high affinity and specificity (11-13). mRNA display enables peptide selection

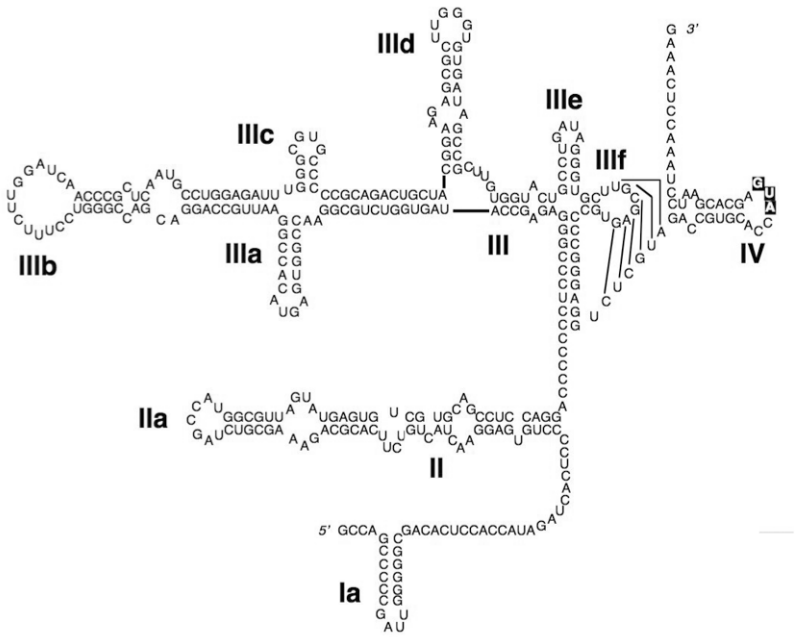

Figure 7.1. Secondary structure of the Hepatitis C Virus internal ribosome entry site (HCV IRES). Domains I-IV are indicated. Translation starts at the AUG codon (boxed) in domain IV. eIF3 binds to domains IIIa and IIIb while the 40S ribosomal subunit binds to domains II, IIIc-f, and IV.

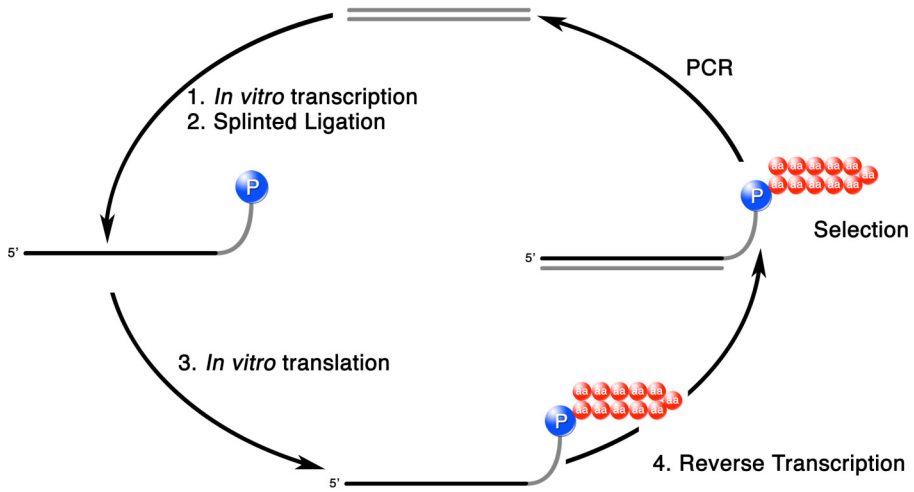

Figure 7.2. An mRNA display selection cycle. A double stranded DNA library is transcribed using T7 RNA polymerase [1] , and the resulting mRNA ligated to a synthetic oligonucleotide containing puromycin [2]. *In vitro* translation of the ligated product results in attachment of a peptide to its encoding mRNA [3]. Reverse transcription generates a cDNA/mRNA hybrid [4], which is used in affinity selection. PCR generates an enriched pool which is used in further cycles of selection.

by covalently linking a peptide to its encoding mRNA (Figure 7.2) (14). We have recently isolated peptides that bind to a catalytically important hairpin from human telomerase RNA, L-P6.1. These peptides were isolated using a reflection selection strategy whereby L-peptides that bind to an L-RNA are first isolated, enabling the synthesis of D-peptides that recognize natural RNA (15, 16). These D-peptides should be more stable against degradation by proteases (17). Thus, we believed that we would be able to use a similar strategy to target domains of the HCV IRES and obtain D-peptides that would inhibit IRES-mediated translation.

We noticed that the HCV IIId hairpin is very similar in sequence to the P6.1 hairpin from telomerase (Figure 7.3). The IIId hairpin contains the same loop sequence, 5'-UUGGG-3', except that it contains an extra 3' U nucleotide (U18, Figure 7.3) that is flipped out of the loop (18, 19). Other RNAs have been observed to extrude loop nucleotides when folding. For example, the *boxB* hairpin contains a pentaloop where the

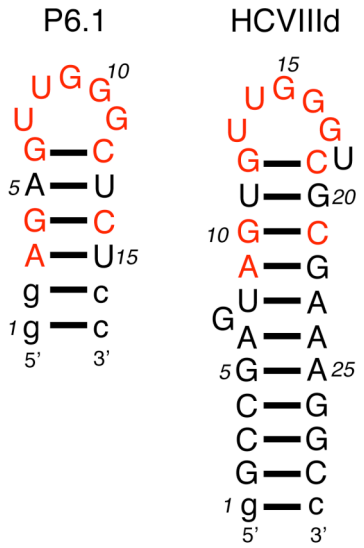

Figure 7.3. RNA models of P6.1 (left) and HCV IIId (right). Nucleotides that are common to both hairpins are colored red while nucleotides added for *in vitro* transcription are shown in lower case.

fourth nucleotide is extruded, resulting in a stable GNRA tetraloop fold (20, 21). Both P6.1 and IIId contain a GU wobble pair at the base of the loop, a GC closing pair, and several common nucleotides in the stem.

The P6.1 hairpin adopts a fold similar to that of UNCG tetraloops, with G10 (Figure 7.3) extruded (22). The HCV IIId hairpin does not exhibit the same conformation as the P6.1 hairpin, however the IIId loop is disordered (18), possibly suggesting structural homogeneity. It is therefore possible that the IIId loop may adopt conformations similar to L-P6.1 (23); upon peptide binding, a different structure would be enforced (24-26).

We were therefore interested to test if the peptides we isolated from the L-P6.1 selection would bind to an L-HCV IIId RNA. If the peptides possessed moderate affinity for L-HCV IIId, we felt that we would be able to then isolate peptides which were specific for either L-HCV IIId or L-P6.1 based on the fact that previous work has shown that RNA binding specificity is determined by a relatively few (2-4) number of mutations (27).

Results and Discussion

We first tested the ability of the pool targeting L-P6.1 to bind to L-HCV IIId. ^{35}S-labeled fusions from round 16 were tested in an *in vitro* binding assay using biotinylated L-HCV IIId as a target. Figure 7.4 shows that the pool binds to both L-P6.1 and to L-HCV IIId, although it prefers the L-P6.1 by a factor of ~1.5-fold.

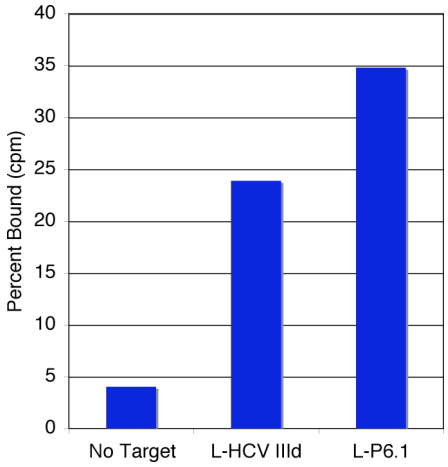

Figure 7.4. Binding of the round 16 pool to L-P6.1 and L-HCV IIId. A sample where target was omitted (no target) is shown as a control.

Previous data (Chapter 6) showed that the pool was composed of three sequence families, which possessed different affinities toward L-P6.1. This suggested that the individual peptide families utilized different binding contacts and it was therefore possible that individual clones would discriminate between L-P6.1 and L-HCV IIId differently. Figure 7.5 shows that representative clones from the L-P6.1 do indeed possess different specificities toward the L-P6.1 and L-IIId targets. Clone 18C1 is highly specific for the L-P6.1 target while 18C17 shows virtually no specificity between the two hairpins. 18C5 shows specificity representative of the pool as a whole; it prefers the L-P6.1 target by approximately twofold.

Improving RNA Binding Specificity

We have previously shown that there are "hot spots" responsible for specificity in RNA binding peptides; as few as four mutations were required to change the binding specificity between the λ N and P22 N peptides (24, 27). We therefore felt that it might

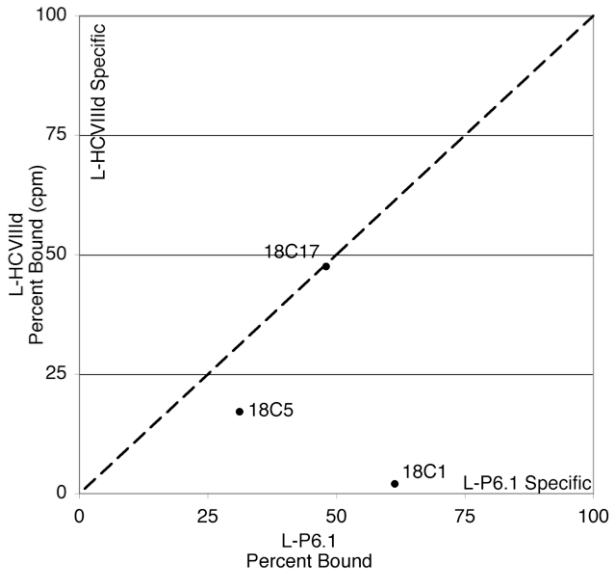

Figure 7.5. Specificities of the individual sequences from the round 18 pool targeting L-P6.1. Individual clones were synthesized as ^{35}S-labeled fusions and tested for binding to immobilized L-HCV IIId and L-P6.1. The x-axis represents L-P6.1 binding while the y-axis represents L-HCV IIId binding. Therefore, peptides in right, lower corner of the graph possess high specificity for the L-P6.1 target. The dotted line shows 1:1 binding.

be possible to isolate specific peptides for each RNA target by introducing mutations in the round 18 pool, then performing additional round of selection on each RNA target.

Mutagenic PCR was performed on the round 18 pool and the resulting molecules sieved against immobilized L-P6.1 or L-HCV IIId. We chose to mutagenize the pool, rather than individual sequences (e.g., mutagenizing 18C1 for the L-P6.1 selection and 18C17 for the L-HCV IIId selection), since it was possible that other functional sequences could have been present at low copy numbers (28). This was more important for the HCV IIId selection since the selective pressure on the pool was changed; weak, low copy L-P6.1 binding sequences could have higher affinity for L-HCV IIId.

A total of three rounds of mutagenic PCR and selection were performed, followed by three more rounds of selection with no mutagenic PCR. Pool binding to L-P6.1 and

L-HCV IIId was monitored by measuring the binding of ^{35}S-labeled fusions against each immobilized RNA target. Figure 7.6 shows the binding of the L-P6.1 selection while Figure 7.7 shows the binding of the L-HCV IIId selection. Both pools showed an initial decrease in binding during rounds that contained mutagenic PCR, then an increase in binding in the subsequent rounds.

As the selection progressed, each pool showed increased specificity for its cognate target, although the L-HCV IIId pool never increased its specificity much more than 1:1 (Figure 7.8). The selection stringency for specificity was increased by addition of a negative selection step where the pool was precleared with immobilized noncognate target (e.g., the L-P6.1 selection was bound to immobilized L-HCV IIId before positive

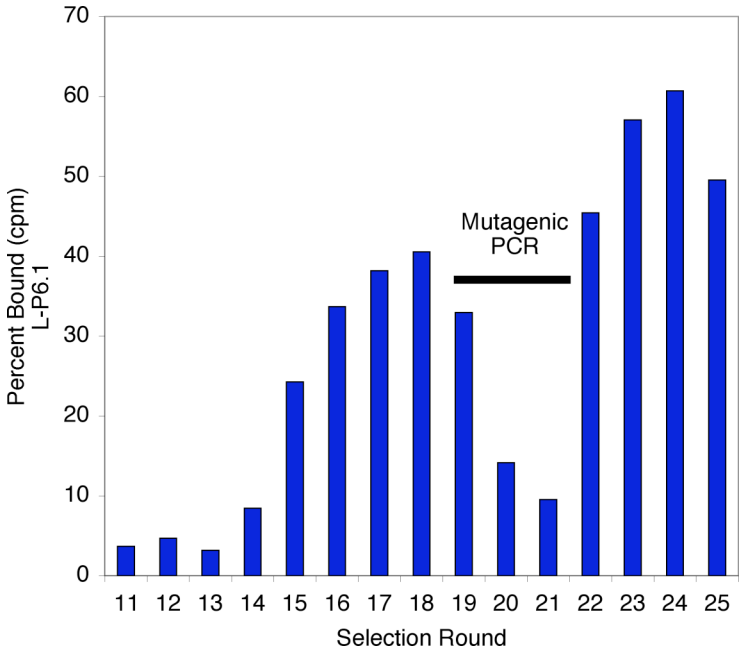

Figure 7.6. Binding of rounds 11-25 of the L-P6.1 selection. Mutagenic PCR was introduced in rounds 19, 20, and 21 resulting in a decrease in pool binding.

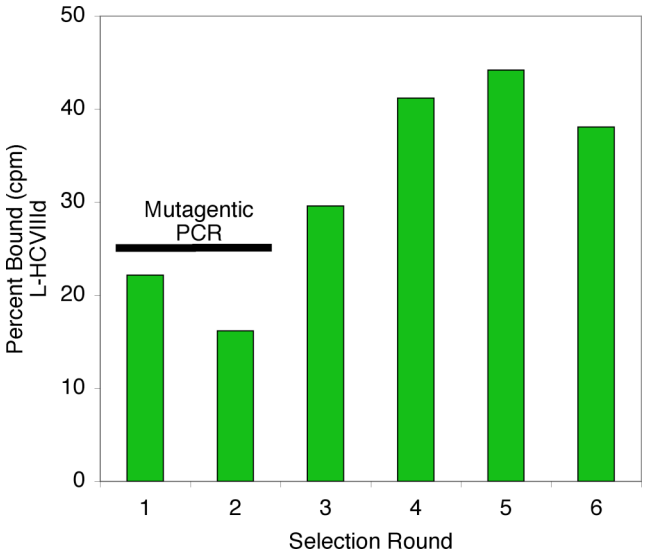

Figure 7.7. Binding of rounds 1-6 of the L-HCV IIId selection. Round 19 from the L-P6.1 selection was subjected to mutagenic PCR, then selected against immobilized L-HCV IIId. Mutagenic PCR was also added to rounds 1 and 2 of the L-HCV selection.

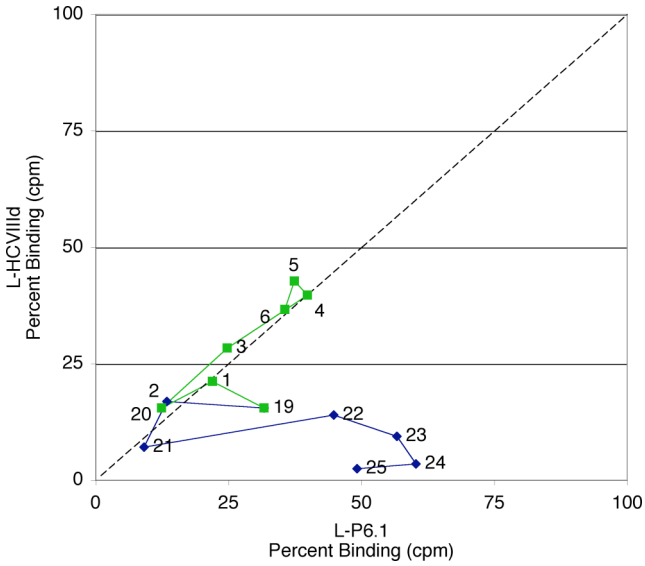

Figure 7.8. The specificity of rounds 0-6 of the L-HCV IIId selection (green) and rounds 19-25 of the L-P6.1 selection (blue). The dotted line represents equal affinities to L-P6.1 and L-HCV IIId. The x-axis represents L-P6.1 binding while the y-axis represents L-HCV IIId binding.

selection against L-P6.1). Additional rounds of selection resulted in no increase in binding and round 24 from the L-P6.1 selection and round five from the L-HCV IIId selection were sequenced.

P6.1 Binding Peptides

Figure 7.9 shows the sequences from the round 24 pool that were selected against L-P6.1. A single family of sequences descended from the 18C1 family dominated the pool; no sequences from the 18C5 family or the 18C17 family were seen. The 18C1 family showed the highest affinity and highest specificity for L-P6.1, explaining why it overtook the round 24 pool.

Clone	Peptide Sequence
	1 10 20 30
Parental Sequence	MMDWKRAKLNRLSVRKLRKYADYFTSGGLRASAI
24C1	MM**V**R**K**R**T**KL**S**RLSVRK**M**RKYADYF**SGS**GLRASAI
24C4	M**S**D**Y**KRAKLNRLSVRKLRKYADYFT**RV**GLRASAI
24C5	-MDWKR**S**KLNRLS**A**RKLRKYADYFTS**S**GLRASAI
24C6	MMDWKR**T**KL**S**RLSVRKLRKYADYFT**GV**GLRASAI
24C7	M**K**DWKR**T**K**FY**RLS**D**RKLRKY**S**DYFTS**V**GLRASAI
24C9	MMDWKR**S**KLNRLSVRKLRKYADYF**AR**GGLRASAI
24C10	M**S**D**S**KRAKLNR**I**S**A**RK**T**RKY**S**DYF**SRV**GLRASAI
Consensus	M-D-KR-KL-RLS-RK-RKY-DYF---GLRASAI

Figure 7.9. Sequences from the round 24 pool targeting L-P6.1. The parental 18C1 is shown above as a reference. Mutations are highlighted in bold text. The 3' primer codes for the amino acid sequence GLRASAI, thereby preventing any mutations from occuring in those positions. A consensus sequence is derived from the peptide sequences.

Assuming that the mutagenic PCR introduced mutations at every position in the template, alignment of the round 24 clones could be used to show positions important for

RNA binding. A consensus sequence of DxKRxKLxRLSxRKxRKYxDYF was generated from the alignment. This sequence explains why attempts to truncate the peptide at position 21 resulted in nonbinding peptides (Chapter 6). No mutations to D22, Y23, or F24 were seen, implying that these positions are important for peptide binding. Additionally, all basic residues (Arg and Lys) are conserved, consistent with the fact that basic charge is important for RNA recognition by peptides.

We then tested the specificity of individual clones toward L-P6.1 and L-HCV IIId using the *in vitro* binding assay (Figure 7.10). Although it was difficult to obtain accurate binding affinities for most of the peptides because of low binding affinities to L-HCV IIId (typically, less than 3%), most of the 24C sequences exhibited similar preferences for L-P6.1 as the parental 18C1 sequence (Figure 7.10B). However, two clones, 24C7 and 24C10, showed an increase in specificity for L-P6.1 of 3-5 fold, as compared to the parental sequence (Figure 7.10B). Both 24C7 and 24C10 contain the A21S mutation, while all other sequences do not, suggesting that this position is a source for the increased specificity exhibited by these peptides. In order to test this hypothesis, we constructed an 18C1 mutant containing the A21S mutation and tested its specificity toward the two hairpins. The single A21S mutation increases the specificity for L-P6.1 from 30-fold to 60-fold (data not shown), showing that it contributes, but is not the sole determinant, of specificity.

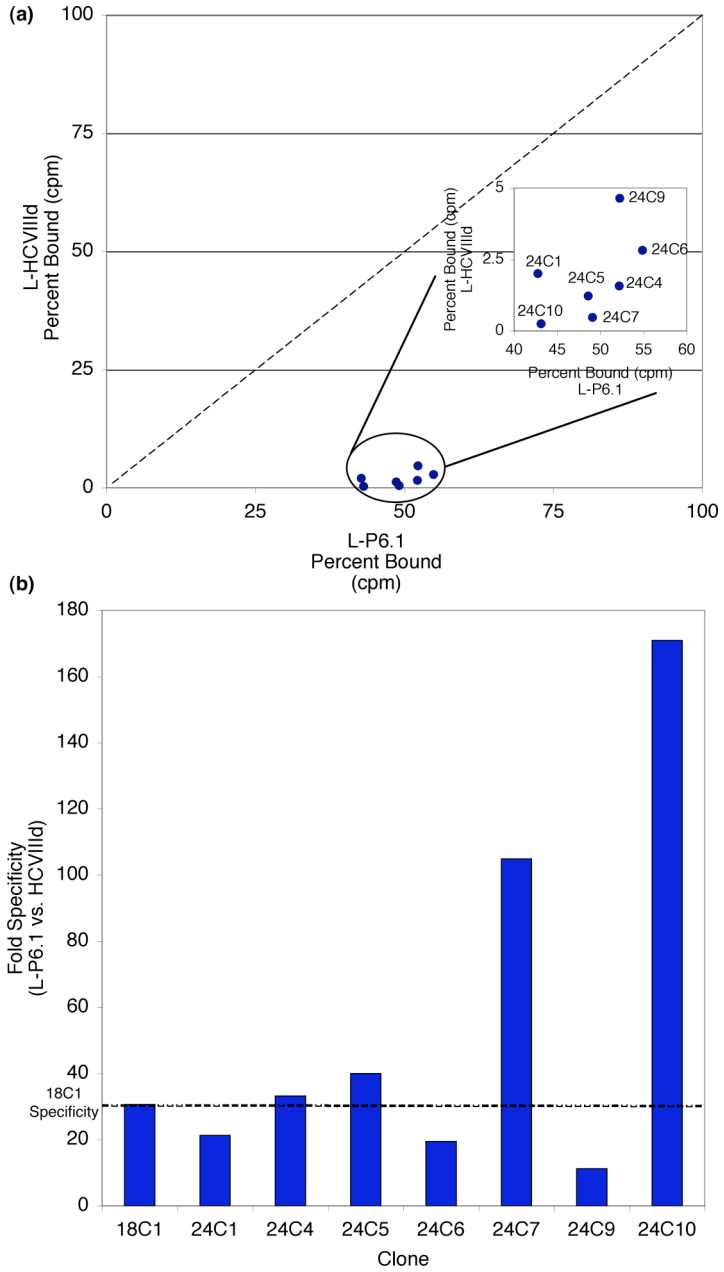

Figure 7.10. Specificity of individual round 24 clones**.** **(a)** The binding of the clones is magnified for clarity (inset). **(b)** Fold specificity of L-P6.1 binding versus L-HCV IIId binding. Higher bars represent more specific L-P6.1 sequences. The specificity of the 18C1 parental sequence is shown by the dotted line.

HCV IIId Binding Peptides

The round 5 pool targeting L-HCV IIId was sequenced and yielded three families of sequences (Figure 7.11). As expected, descendents from the 18C17 sequence, which had shown little selectivity for L-P6.1 or L-HCV IIId, were present, and the 18C1 and 18C5 sequences, which preferred L-P6.1, were absent. Two new families not seen in the original 18C pool were also isolated, supporting our decision to randomize the entire pool rather than the 18C17 sequence. Little sequence similarity is seen between the three families, preventing any consensus sequence from being deduced.

Clone	Peptide Sequence
	1 10 20 30
Parental Sequence	MKHSNSSRGRKTLWRALTLWLLMQSLKRTSGGLRASAI
HCV5-2	MK**L**P**N**SSRGRKTLWRA**M**TLWLLMQSL**Q**RTSGGLRASAI
HCV5-9	MK**Y**SNSSRGRKTLWRALTLWLLMQSLKRTS**D**GLRASAI
HCV5-10	MK**Y**SNSSRGRKTLWR**GW**TLWIL**I**QSLKRT**RD**GLRASAI
HCV5-1	MNTLKELVLLYLSERRGL**S**VSKADFLK**R**TSDGLRASAI
HCV5-5	MN**S**LKELVLLYL**R**ERRGLPVSKPDF**A**KW**V**KDGLRASAI
HCV5-8	MNTLKELVLLYLSE**Q**RGLP**I**SKSDFL**R**WTRGGLRASAI
HCV5-7	MMKRFSAKVSTLSRERRRMLRTLIQRRLTGGGLRASAI

Figure 7.11. Sequences from the round 5 pool targeting L-HCV IIId. The parental sequence (18C17) for HCV5-2, 9, and 10 is shown above as a reference. Peptides are grouped into three sequence families. Muations are highlighted in bold text.

Additionally, the sequences contain fewer mutations per template when compared to the round 24 sequences from the L-P6.1 selection. An average of ~5.5 mutations per template were seen round 24 of the L-P6.1 selection while only ~3.5

mutations were template occurred in the L-HCV IIId selection. Although a difference in error rates could be a possible explanation, the fact that both mutagenesis experiments were performed in parallel under the same experimental conditions argues against this hypothesis. Instead, a more plausible explanation is that more positions are required for binding for the sequence families from the L-HCV IIId selection than from the L-P6.1 selection.

Figure 7.12 shows the binding specificity of the round five clones as determined by the *in vitro* binding assay. Two clones, HCV5-1 and HCV5-7 bind the L-HCV IIId

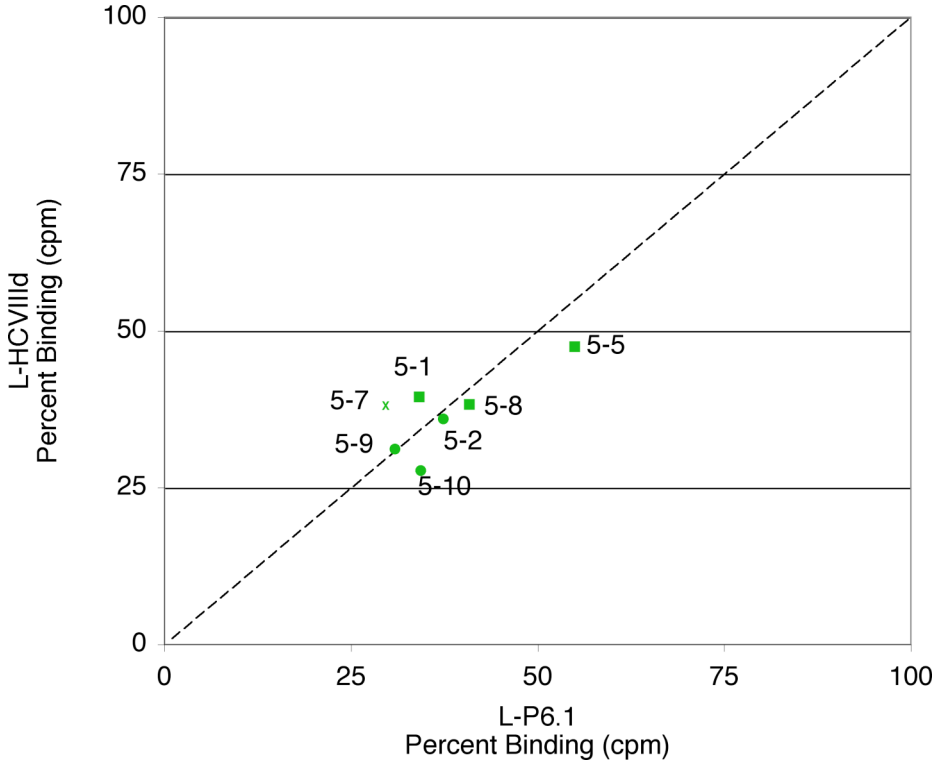

Figure 7.12. Specificity of individual round 5 clones targeting L-HCV IIId. Peptides belong to three sequence families (Figure 7.11) and families 1, 2, and 3 are denoted by circles, squares, and crosses, respectively.

hairpin with higher affinity than the L-P6.1 hairpin. Even these clones, however, lack the ability to effectively discriminate between the two hairpins; the entire pool exhibits little specificity for either hairpin.

It is worth noting that the two sequences that bind L-HCV IIId better than L-P6.1, HCV5-1 and HCV5-7, belong to peptide families that were not seen in round 18. It therefore must be much easier to enrich for a novel sequence family than it is to endow a degenerate sequence with more specificity; there are more unique sequences in the pool than there are multiple mutations conferring specificity.

Conclusions

Starting from a pool of sequences that bound L-P6.1, we have isolated sequences that bind to L-P6.1 and L-HCV IIId. We attempted to increase the selectivity of the peptides for each target by including mutagenic PCR in the selection cycle, however we were only successful in isolating L-P6.1-specific sequences.

Although only a few (2-4 mutations) mutations can result in specificity changes, these mutations must be relatively rare. For example, in order to search all possible combinations of twenty amino acids at two positions in a sequence of n length, there will be $200 \times \left(n^2 - n\right)$ sequences. Therefore, a total of ~1.4×10^5 two-position mutations are possible for the X27S library. Additionally, there are other factors that make it more difficult to search sequence space for highly specific mutants. Mutagenic PCR is heavily biased towards certain mutations, and the degeneracy of the genetic code prevents many mutations from occurring by a one-nucleotide change.

These data suggest that there are two possible alternatives to isolate more specific L-HCV binding peptides. First, returning to an earlier round (e.g., round 12) and reselecting against the L-HCV target may yield more unique peptides with higher affinities toward L-HCV IIId. Such a strategy also has the advantage of not requiring negative selection steps to remove L-P6.1 binding sequences. Secondly, doping several of the round 5 HCV IIId-binding sequences and reselecting against immobilized L-HV IIId would be a more effective strategy than utilizing mutagenic PCR in the selection cycle. Our data argue that mutations increasing specificity are relatively rare, resulting in the need for higher mutagenesis rates and more cycles of selection. Doping the sequences will also result in less mutational bias and access to all twenty amino acids at a single position, rather than mutations resulting from a one-base change. Future experiments will show if it is possible to isolate peptides with increased specificity.

Materials and Methods

In Vitro Selection

The selection was performed as described in Chapter 6, for the L-P6.1 selection rounds (pg. 149).

Mutagenic PCR

PCR conditions were the same as the selection rounds, except the dNTP concentrations were 1 mM of dCTP and dTTP and 0.2 mM of dATP and dGTP, the $MgCl_2$ concentration was increased to 7 mM, and $MnCl_2$ was added to a final concentration of 0.5 mM. Samples were cycled for 1 minute at 94 ºC, 1 minute at 55 ºC, and 2 minutes at 72 ºC. After every four cycles, 10 μL of PCR reaction was transferred to 90 μL of fresh buffer, dNTPs, primers and Taq heated to 72 ºC. This process was repeated for up to 15 transfers. Samples from different cycles were pooled and used for the next round of selection. The mutagenic rates for the first, second, and third mutagenic PCR reactions were an average of 0.031 mutations/codon (1 amino acid change per template), 0.055 mutations/codon (1.8 aa changes/template), and 0.057 mutations/codon (1.9 aa changes/template).

In Vitro Binding Assay

dT-purified ^{35}S-labeled fusions (~100,000 cpm) were incubated with 0.1-0.2 μM immobilized, annealed RNA target (50 μL of a 50/50 (v/v) slurry) in binding buffer with 50 μg/mL tRNA for one hour at 4 ºC. The samples were transferred to Spin-X columns

(Costar) and washed three times with 700 μL of binding buffer. The supernatant, washes, and beads counted by scintillation.

RNA Synthesis

Biotinylated L-HCV IIId RNA (5-GGCCGAGUAGUGUUGGGUCGCGAAAGGC CAAA-biotin-3') was synthesized and deprotected by Chemgenes. RNA was gel purified by 20% urea-PAGE, electroeluted, and ethanol precipitated.

Sequencing

Pool templates were PCR amplified, gel purified using the QiaQuick gel extraction kit (Qiagen), and cloned using a TOPO-TA cloning kit (Invitrogen). Single colonies were grown in LB broth containing 50-100 μg/mL Ampicillin, and purified using the QiaPrep Spin Miniprep kit (Qiagen). Sequences were analyzed by Sequencher.

References

1. Cohen, J. The scientific challenge of hepatitis C. (1999) *Science* **285**, 26-30.
2. Tan, S.L., He, Y., Huang, Y. and Gale, M., Jr. Strategies for hepatitis C therapeutic intervention: now and next. (2004) *Curr Opin Pharmacol* **4**, 465-470.
3. Honda, M., Beard, M.R., Ping, L.H. and Lemon, S.M. A phylogenetically conserved stem-loop structure at the 5' border of the internal ribosome entry site of hepatitis C virus is required for cap-independent viral translation. (1999) *J Virol* **73**, 1165-1174.
4. Kieft, J.S., Zhou, K., Jubin, R. and Doudna, J.A. Mechanism of ribosome recruitment by hepatitis C IRES RNA. (2001) *Rna* **7**, 194-206.
5. Gallego, J. and Varani, G. The hepatitis C virus internal ribosome-entry site: a new target for antiviral research. (2002) *Biochem Soc Trans* **30**, 140-145.
6. Lytle, J.R., Wu, L. and Robertson, H.D. Domains on the Hepatitis C virus internal ribosome entry site for 40s subunit binding. (2002) *Rna* **8**, 1045-1055.
7. Spahn, C.M., Kieft, J.S., Grassucci, R.A., Penczek, P.A., Zhou, K., Doudna, J.A. and Frank, J. Hepatitis C virus IRES RNA-induced changes in the conformation of the 40s ribosomal subunit. (2001) *Science* **291**, 1959-1962.
8. Collier, A.J., Gallego, J., Klinck, R., Cole, P.T., Harris, S.J., Harrison, G.P., Aboul-Ela, F., Varani, G. and Walker, S. A conserved RNA structure within the HCV IRES eIF3-binding site. (2002) *Nat Struct Biol* **9**, 375-380.

9. Kieft, J.S., Zhou, K., Grech, A., Jubin, R. and Doudna, J.A. Crystal structure of an RNA tertiary domain essential to HCV IRES-mediated translation initiation. (2002) *Nat Struct Biol* **9**, 370-374.

10. Toulme, J.J., Darfeuille, F., Kolb, G., Chabas, S. and Staedel, C. Modulating viral gene expression by aptamers to RNA structures. (2003) *Biol Cell* **95**, 229-238.

11. Barrick, J.E., Takahashi, T.T., Ren, J., Xia, T. and Roberts, R.W. Large libraries reveal diverse solutions to an RNA recognition problem. (2001) *Proc Natl Acad Sci U S A* **98**, 12374-12378.

12. Barrick, J.E., Takahashi, T.T., Balakin, A. and Roberts, R.W. Selection of RNA-binding peptides using mRNA-peptide fusions. (2001) *Methods* **23**, 287-293.

13. Xia, T., Frankel, A., Takahashi, T.T., Ren, J. and Roberts, R.W. Context and conformation dictate function of a transcription antitermination switch. (2003) *Nat Struct Biol* **10**, 812-819.

14. Takahashi, T.T., Austin, R.J. and Roberts, R.W. mRNA display: ligand discovery, interaction analysis and beyond. (2003) *Trends Biochem Sci* **28**, 159-165.

15. Schumacher, T.N., Mayr, L.M., Minor, D.L., Jr., Milhollen, M.A., Burgess, M.W. and Kim, P.S. Identification of D-peptide ligands through mirror-image phage display. (1996) *Science* **271**, 1854-1857.

16. Williams, K.P., Liu, X.H., Schumacher, T.N., Lin, H.Y., Ausiello, D.A., Kim, P.S. and Bartel, D.P. Bioactive and nuclease-resistant L-DNA ligand of vasopressin. (1997) *Proc Natl Acad Sci U S A* **94**, 11285-11290.

17. Eckert, D.M., Malashkevich, V.N., Hong, L.H., Carr, P.A. and Kim, P.S. Inhibiting HIV-1 entry: discovery of D-peptide inhibitors that target the gp41 coiled-coil pocket. (1999) *Cell* **99**, 103-115.

18. Lukavsky, P.J., Otto, G.A., Lancaster, A.M., Sarnow, P. and Puglisi, J.D. Structures of two RNA domains essential for hepatitis C virus internal ribosome entry site function. (2000) *Nat Struct Biol* **7**, 1105-1110.

19. Klinck, R., Westhof, E., Walker, S., Afshar, M., Collier, A. and Aboul-Ela, F. A potential RNA drug target in the hepatitis C virus internal ribosomal entry site. (2000) *Rna* **6**, 1423-1431.

20. Legault, P., Li, J., Mogridge, J., Kay, L.E. and Greenblatt, J. NMR structure of the bacteriophage lambda N peptide/*boxB* RNA complex: recognition of a GNRA fold by an arginine-rich motif. (1998) *Cell* **93**, 289-299.

21. Scharpf, M., Sticht, H., Schweimer, K., Boehm, M., Hoffmann, S. and Rosch, P. Antitermination in bacteriophage lambda. The structure of the N36 peptide-boxB RNA complex. (2000) *Eur J Biochem* **267**, 2397-2408.

22. Leeper, T., Leulliot, N. and Varani, G. The solution structure of an essential stem-loop of human telomerase RNA. (2003) *Nucleic Acids Res* **31**, 2614-2621.

23. Leulliot, N. and Varani, G. Current topics in RNA-protein recognition: control of specificity and biological function through induced fit and conformational capture. (2001) *Biochemistry* **40**, 7947-7956.

24. Austin, R.J., Xia, T., Ren, J., Takahashi, T.T. and Roberts, R.W. Differential modes of recognition in N peptide-*boxB* complexes. (2003) *Biochemistry* **42**, 14957-14967.

25. Menger, M., Eckstein, F. and Porschke, D. Dynamics of the RNA hairpin GNRA tetraloop. (2000) *Biochemistry* **39**, 4500-4507.

26. Barrick, J.E. and Roberts, R.W. Achieving specificity in selected and wild-type N peptide-RNA complexes: the importance of discrimination against noncognate RNA targets. (2003) *Biochemistry* **42**, 12998-13007.

27. Austin, R.J., Xia, T., Ren, J., Takahashi, T.T. and Roberts, R.W. Designed arginine-rich RNA-binding peptides with picomolar affinity. (2002) *J Am Chem Soc* **124**, 10966-10967.

28. Bartel, D.P. and Szostak, J.W. Isolation of new ribozymes from a large pool of random sequences. (1993) *Science* **261**, 1411-1418.